




Enhanced Nernst effect above T_c in the quasi-two-dimensional iron pnictide superconductor $\text{CsCa}_2\text{Fe}_4\text{As}_4\text{F}_2$

Miaocong Li ^{1,2}, Zhicheng Wang ¹, Dan Zhao,³ Yabin Liu,¹ Chenxi Jiang,^{1,2} Tao Wu,^{3,4,5} Qian Tao,^{1,*} Guang-Han Cao,^{1,2,5} and Zhu-An Xu ^{1,2,5,†}


¹Zhejiang Province Key Laboratory of Quantum Technology and Device,
Department of Physics, Zhejiang University, Hangzhou 310027, China

²State Key Laboratory of Silicon Materials, Zhejiang University, Hangzhou 310027, China

³Hefei National Laboratory for Physical Sciences at the Microscale and Department of Physics, and Key Laboratory of Strongly-Coupled Quantum Matter Physics, Chinese Academy of Sciences, University of Science and Technology of China, Hefei, Anhui 230026, China

⁴CAS Center for Excellence in Superconducting Electronics (CENSE), Shanghai 200050, China

⁵Collaborative Innovation Centre of Advanced Microstructures, Nanjing University, Nanjing 210093, China

 (Received 19 September 2021; revised 26 January 2022; accepted 2 March 2022; published 28 March 2022)

As a new type of iron pnictide superconductors, $\text{CsCa}_2\text{Fe}_4\text{As}_4\text{F}_2$, featured by its unique FeAs bilayer, presents a quasi-two-dimensional characteristic which distinguishes itself from other iron pnictides. Here we systematically investigated its transport properties and thermoelectric effects, including the Seebeck and Nernst effect, and NMR. An unusual hump in the Nernst coefficient is observed as temperature decreases below 90 K, far above its T_c of 28.5 K. Simultaneously there is a suppression in the Hall coefficient as well as the nuclear spin-lattice relaxation rate in the same temperature range. To clarify this phenomenon, we comparatively investigated two other similar iron-based pnictide superconductors, $\text{Ba}_{1-x}\text{K}_x\text{Fe}_2\text{As}_2$ and $\text{CaKFe}_4\text{As}_4$. Our work indicates there could exist an incoherence-coherence crossover or a kind of Cooper pairing precursor in $\text{CsCa}_2\text{Fe}_4\text{As}_4\text{F}_2$ before achieving its superconductivity, which is different from other iron-based high- T_c superconductors. Such a comparative study may help us to understand the effect of dimensional evolution from three dimensional to two dimensional on high- T_c superconductivity.

DOI: [10.1103/PhysRevB.105.104512](https://doi.org/10.1103/PhysRevB.105.104512)

I. INTRODUCTION

Since the discovery of the iron-based superconductor $\text{LaFeAsO}_{1-x}\text{F}_x$ (so called “1111”-type structure) in 2008 [1], lots of new structure types of pnictide superconductors have been reported, including the “1111”-, “111”-, and “122”-type [2,3]. Recently, a new structure of iron-based superconductor $\text{CsCa}_2\text{Fe}_4\text{As}_4\text{F}_2$, namely, “12442” type was discovered [4]. It can be regarded as the intergrowth of 122- and 1111-type structures, where the 1111-type block is inserted between the Cs atom and the Fe_2As_2 layer. It is hole-type self-doped with a nominal doping level of 0.25 hole/Fe and contains double Fe_2As_2 layers in a unit cell. The two conducting Fe_2As_2 layers are separated by an insulating Ca_2F_2 layer, which makes it quite quasi two dimensional, and thus this 12442-type structure is apparently unique and different from other iron pnictides. Previous electrical transport measurements have revealed its giant anisotropy in resistivity between the ab plane and c axis direction [5,6], and an extremely high upper critical field in the ab plane [7]. Speaking to its electronic structure, angle-resolved photoemission spectroscopy (ARPES) experiments have identified the phenomenon of band splitting induced by this bilayer structure, which is the first

observation in iron-based superconductors [8]. The analogous phenomenon has previously been observed in the “2212”-type cuprate $\text{Bi}_2\text{Sr}_2\text{CaCu}_2\text{O}_{8+\delta}$ [9]. Furthermore, recent neutron scattering experiments have found two-dimensional (2D) spin resonances and revealed a downward dispersion, which resembles the dispersion observed in the hole-doped cuprates and cannot be explained by the theory based on s -wave pairing symmetry [10]. These results imply that the 12442-type iron-based pnictides may share some similar features as the cuprates, which is believed to be intimately related to the unique quasi-two-dimensional structure.

As is well known, dimensionality has a remarkable impact on superconducting properties and there are several ways to achieve two-dimensional superconductors. A widely used way is to grow epitaxially thin films on suitable substrates, and a successful example is the monolayer FeSe thin films on SrTiO_3 . A much larger superconducting gap in monolayer FeSe films, compared to the bulk FeSe, was observed by the scanning tunneling spectra (STS) [11], which promises a higher T_c around 77 K, and was confirmed by the ARPES [12,13]. Another way is to fulfill the quasi-2D structure by increasing the distance between the crucial conducting layers, such as the organic ion intercalated superconductors $(\text{CTA})_x\text{FeSe}$ [14] and $(\text{TBA})_x\text{FeSe}$ [15]. In these cluster-intercalated iron-based materials, the evidence to support preformed Cooper pairs above T_c was found in the recent measurements of NMR and Nernst effect [16]. These unusual

*tao@zju.edu.cn

†zhuan@zju.edu.cn

features induced by the two-dimensional structure can provide insights into understanding the role played by dimensionality in the high- T_c superconductors.

Thermoelectric effects, including the Seebeck and Nernst effect, are sensitive to the electronic structure and the low-energy excitations. The Nernst effect measurements have revealed strong superconducting phase fluctuations above T_c in high- T_c cuprates [17]. In iron-based pnictides, the anisotropy of the Nernst effect is utilized to study the nematic phase [18,19], spin density wave [20], and the evolution of the intermediate phase under pressure [21]. Moreover, recent experiments have exhibited a spontaneous Nernst effect in $\text{Fe}_{1+y}\text{Te}_{1-x}\text{Se}_x$, implying the possibility of locally time-reversal symmetry breaking [22]. Therefore, we propose that the measurements of thermoelectric effects could help understand the unique properties of 12442-type materials that should have a characteristic of reduced dimensionality.

In this paper, we carefully investigated the electrical transport properties, thermoelectric effects, and NMR simultaneously. We observed several unusual features which should be associated with the quasi-2D nature of 12442-type systems. There may exist a large regime of vortex liquid state revealed by the vortex-flowing Nernst effect below T_c . As for temperature above T_c , there is a significant drop in the Hall coefficient and an obvious broad hump in the Nernst coefficient as the temperature cools down below about 90 K. To clarify its origin and explore its relation with dimensionality, we also measured two other similar layered pnictide superconductors $\text{Ba}_{1-x}\text{K}_x\text{Fe}_2\text{As}_2$ (122 type) and $\text{CaKFe}_4\text{As}_4$ (“1144” type) for comparison. These two superconductors are both more three-dimensional, and the 1144-type compound contains the same FeAs bilayer as in the 12442 type. However, the 1144 type is distinguished from the 12442 type by lacking the insulating Ca_2F_2 layer between the two FeAs bilayers. The vortex liquid regime in $\text{Ba}_{1-x}\text{K}_x\text{Fe}_2\text{As}_2$ and $\text{CaKFe}_4\text{As}_4$ is much narrower, implying the close relationship between the vortex liquid state and quasi-two-dimensional structure. Compared with the NMR experiments, we argued that the unusual features observed in both the Nernst effect and the Hall coefficient of 12442 type may be caused by a kind of precursor which represents an incoherent-coherent crossover or even preformed Cooper pairs. Such kind of precursor has also been proposed and discussed in the monolayer FeSe thin films and molecular-intercalated FeSe systems, and a common character of these systems is the quasi-two-dimensional nature.

II. EXPERIMENTAL DETAILS

Single crystals of these three type samples are all grown by a self-flux method and the details are reported previously [5,23,24]. All the transport measurements are carried out on a Quantum Design physical property measurement system (PPMS-DynaCool) and/or an Oxford-15T cryostat. The standard six-terminal method was used in resistivity and Hall effect measurements. As for the measurements of thermoelectric effect, a resistor of 1000 Ω is utilized as the heater to establish the thermal gradient. The E-type thermocouple is used to measure the temperature differences across the samples. In the measurements of the Hall and Nernst effect, the

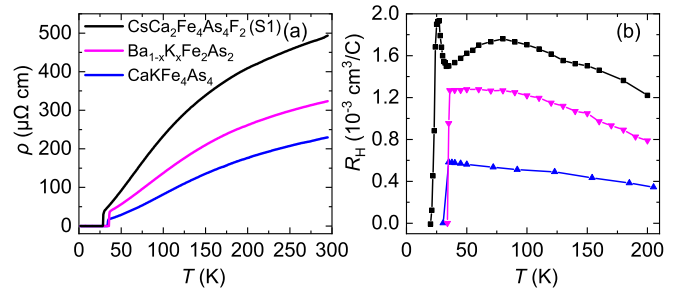


FIG. 1. Temperature dependence of (a) resistivity and (b) Hall coefficient of $\text{CsCa}_2\text{Fe}_4\text{As}_4\text{F}_2$, $\text{Ba}_{1-x}\text{K}_x\text{Fe}_2\text{As}_2$, and $\text{CaKFe}_4\text{As}_4$. Different colors: black, magenta, and blue represent $\text{CsCa}_2\text{Fe}_4\text{As}_4\text{F}_2$, $\text{Ba}_{1-x}\text{K}_x\text{Fe}_2\text{As}_2$, and $\text{CaKFe}_4\text{As}_4$, respectively.

magnetic field was swept from positive to negative direction to eliminate the misalignment of transverse electrical contacts. The Nernst effect measurements of $\text{CsCa}_2\text{Fe}_4\text{As}_4\text{F}_2$ were conducted on two different pieces of samples, which are named S1 and S2, in order to rule out possible accident signals. All the other data of the transport measurements were collected from the samples cut from the same crystal or batch for each system. The maximum magnetic field in the Hall measurement and Nernst effect for S1 is 3 T and 8 T, respectively.

The NMR measurements were performed on the ^{75}As nuclei whose nuclear spin number is 3/2 and the gyromagnetic ratio for bare nuclei is 7.2919 MHz/T. The standard NMR spin-echo technique was applied with a commercial NMR spectrometer from Thamway Co. Ltd. The external magnetic field $B = 12$ T is applied to the c axis of $\text{CsCa}_2\text{Fe}_4\text{As}_4\text{F}_2$ single crystal and generated by a 12 T magnet from Oxford Instruments. There are two types of As sites, namely, the As1 site which is close to the Cs plane and the As2 site which is close to the Ca_2F_2 block.

III. RESULTS AND DISCUSSION

Figure 1(a) shows the temperature dependence of resistivity for the three samples, i.e., 12442, 1144, and 122 type. The obtained superconducting temperature, which is defined as the zero-resistance temperature, is 28.5, 33.9, and 35.6 K for the 12442-, 1144-, and 122-type samples, respectively, and they are qualitatively consistent with the literatures [5,25–27]. By comparing the shapes of the resistivity curves, it can be found that all exhibit a convex behavior upon cooling. Such a convex temperature dependence of resistivity is often observed in hole-type 122-type superconductors [28,29]. In addition, the temperature dependence of the elastoresistance is similar among the three systems [30], indicating the comparison of these three materials is appropriate. Another interesting feature in resistivity is that the temperature dependence of resistivity becomes almost linear as the temperature is below about 90 K for $\text{CsCa}_2\text{Fe}_4\text{As}_4\text{F}_2$, which is consistent with the literature [5]. In the previous studies, it has been found that, as the doping level is around the optimal doping, the temperature dependence of resistivity will usually be close to the linear dependence in 122-type pnictides [28,29,31]. From this viewpoint, $\text{CsCa}_2\text{Fe}_4\text{As}_4\text{F}_2$ is in the nearly optimally doped region. In addition, it has been confirmed by the ARPES experiment

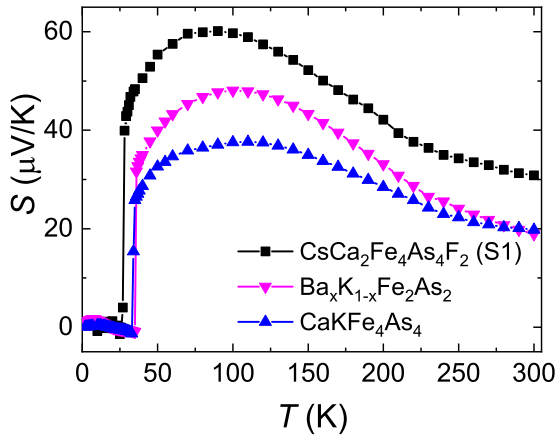


FIG. 2. Temperature dependence of Seebeck coefficients of $\text{CsCa}_2\text{Fe}_4\text{As}_4\text{F}_2$, $\text{Ba}_{1-x}\text{K}_x\text{Fe}_2\text{As}_2$, and $\text{CaKFe}_4\text{As}_4$, indicated by black, magenta, and blue symbols, respectively.

recently that the hole density is about 0.25 hole/Fe in the related compound, i.e., $\text{KCa}_2\text{Fe}_4\text{As}_4\text{F}_2$ [8]. All these results are consistent with the nominal doping level in $\text{CsCa}_2\text{Fe}_4\text{As}_4\text{F}_2$, which suggests it could be in the slightly overdoped region.

Figure 1(b) displays the temperature dependence of the Hall coefficient. All the Hall coefficients of three systems are positive, suggesting that the hole-type charge carriers are dominant. However, the three samples exhibit some different features in the Hall coefficient. Let us focus on the behavior of $\text{CsCa}_2\text{Fe}_4\text{As}_4\text{F}_2$, which is the most unusual one among them. There is a slope change at the temperature around 80 K, which qualitatively agrees with the hump detected in the Nernst effect [shown in Fig. 3(c)] and will be discussed with the Nernst effect in detail later. In addition to this, as the temperature decreases close to T_c , a jump emerges and then the

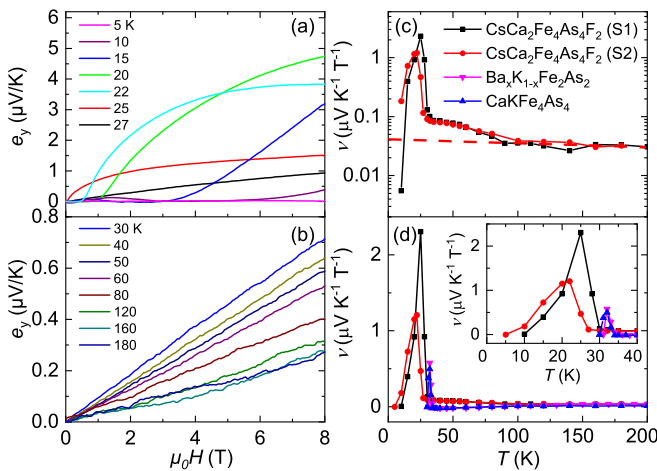


FIG. 3. (a) and (b) stand for the Nernst effects of $\text{CsCa}_2\text{Fe}_4\text{As}_4\text{F}_2$ at various temperatures by sweeping the magnetic field. Temperature range is below T_c in (a) and above T_c in (b). (c) Nernst coefficients of two different pieces of samples with logarithmic coordinates. Red dashed line represents the background. (d) Comparison of three different materials' Nernst coefficients. Inset: enlarged plot for temperature below 40 K.

coefficient drops to zero eventually as the sample enters the superconducting state. Such a jump around T_c is not observed for the other two systems. Since a large regime of vortex liquid state has been observed in this 12442-type material through the measurement of irreversible field [5], this phenomenon of Hall coefficient might be related to the vortex movement. Once the temperature is close to T_c , by applying a magnetic field, the vortex begins to move, which contributes to the Hall coefficient, as a result. As the temperature continuously decreases, the irreversible field becomes larger, therefore the vortex is pinned and the Hall coefficient drops quickly to zero. A similar vortex Hall effect near T_c has been reported in the hole-doped cuprate superconductor $\text{La}_{2-x}\text{Sr}_x\text{CuO}_4$ [32]. As for the other two superconductors, different behavior is observed. The Hall coefficient of $\text{CaKFe}_4\text{As}_4$ remains increasing upon cooling and then drops to zero quickly as it becomes superconducting, consistent with the previous report [25]. For $\text{Ba}_{1-x}\text{K}_x\text{Fe}_2\text{As}_2$, the behavior is similar to $\text{CaKFe}_4\text{As}_4$ at high temperature, but below 80 K, it presents a tendency of saturation. Comparing the temperature dependence of the Hall coefficient and T_c with the literatures [26,27], it is suggested that $\text{Ba}_{1-x}\text{K}_x\text{Fe}_2\text{As}_2$ is in the moderately overdoped region, possibly $x \sim 0.45$.

Speaking to the Seebeck coefficients shown in Fig. 2, the thermopower is all positive, consistent with the Hall coefficient. The signal drops to zero at their superconducting transition temperature T_c , corresponding with the resistivity measurements, albeit a little lower, which may be due to the slight sample heating in the thermal measurements. The thermopower of the three systems exhibits similar temperature dependence, like in resistivity, and no anomaly has been observed.

The Nernst effect of $\text{CsCa}_2\text{Fe}_4\text{As}_4\text{F}_2$ is presented in Figs. 3(a) and 3(b), below and above T_c , respectively. The signals of the Nernst effect are nonlinear in the superconducting state, which is a feature of the vortex-flowing induced Nernst signals. Below 5 K, the Nernst signals drop to zero because the vortex lattice becomes solid and pinned. In an intermediate temperature regime around T_c , the Nernst signals start to increase quickly once the magnetic field exceeds its depinning field and the vortices begin to move. As the temperature increases much above T_c , the Nernst signals become linear with the magnetic field. Upon further increasing temperature, more than 90 K, the temperature dependence of Nernst signals becomes very weak. The Nernst coefficient is deduced and plotted in Fig. 3(c). It is defined as the initial slope for the temperature below T_c . As for above T_c , it is the slope of the magnetic field dependent curve. The Nernst coefficient almost coincides with each other for two pieces of samples, S1 and S2, which indicates that this behavior of the Nernst effect should be intrinsic and repeatable for $\text{CsCa}_2\text{Fe}_4\text{As}_4\text{F}_2$.

It can be noticed that the Nernst signal is still large in a wide temperature region below T_c until it goes down to zero, reminiscent of the large vortex-flowing regime in $\text{LaO}_{0.9}\text{F}_{0.1}\text{FeAs}$ [33]. This phenomenon implies the vortex motion exists even at very low temperatures, which agrees well with the aforementioned Hall effect data and suggests a large vortex liquid regime due to the quasi-2D nature of this system. As for the temperatures above T_c up to 90 K,

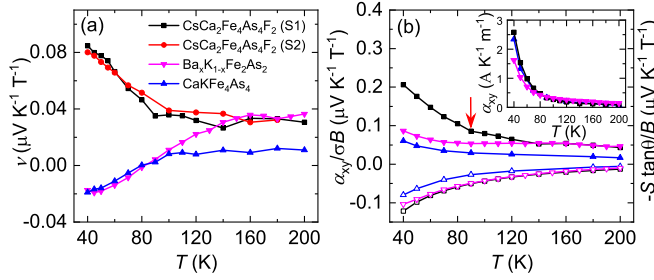


FIG. 4. (a) Temperature dependence of Nernst coefficients in the temperature range of 40–200 K. (b) Temperature dependence of $\alpha_{xy}/\sigma B$ and $-S \tan \theta/B$, represented by solid and hollow marks, respectively. The inset of (b) is the temperature evolution of the off-diagonal Peltier coefficient α_{xy} . The red arrow in (b) indicates the deviation of origin behavior.

an unusual hump in the Nernst coefficient is observed, far away from its T_c , which also coincides with the slope change in the Hall coefficient. Above 90 K, there is the background marked by the red dashed line although the Nernst signals are still large compared to usual metals or superconductors, which may result from its multiband electronic structure.

In order to understand the abnormal Nernst effect above T_c , the Nernst effect of two similar layered pnictide superconductors, $\text{Ba}_{1-x}\text{K}_x\text{Fe}_2\text{As}_2$ and $\text{CaKFe}_4\text{As}_4$, were measured and their data are plotted together with $\text{CsCa}_2\text{Fe}_4\text{As}_4\text{F}_2$ in Fig. 3(d). Visibly, the Nernst effect behaviors of the three systems are significantly different. Below T_c , a sharp peak in the Nernst coefficients of $\text{Ba}_{1-x}\text{K}_x\text{Fe}_2\text{As}_2$ and $\text{CaKFe}_4\text{As}_4$ is observed from the inset figure of Fig. 3(d), which is contrary to $\text{CsCa}_2\text{Fe}_4\text{As}_4\text{F}_2$, demonstrating that the vortices are quickly pinned below T_c for the former two systems, in accord with the results of the Hall effect. This comparison implies that $\text{Ba}_{1-x}\text{K}_x\text{Fe}_2\text{As}_2$ and $\text{CaKFe}_4\text{As}_4$ are more three-dimensional superconductors, and reconfirms that $\text{CsCa}_2\text{Fe}_4\text{As}_4\text{F}_2$ is quasi-two-dimensional [5]. For a better view of the Nernst effect in higher temperatures (above T_c), i.e., for the temperature range between 40 and 200 K, an enlarged plot of Nernst data is shown in Fig. 4(a). As the temperature is slightly above T_c , the Nernst signals of $\text{Ba}_{1-x}\text{K}_x\text{Fe}_2\text{As}_2$ and $\text{CaKFe}_4\text{As}_4$ are negative and increase to positive slowly upon warming around 80 K. The sign change of the Nernst effect is often observed in multiband metals. In contrast, the Nernst signals of $\text{CsCa}_2\text{Fe}_4\text{As}_4\text{F}_2$ remain always positive and remarkably larger than that of the other two systems; for instance, almost two to four times larger around 90 K.

To further elucidate this abnormal Nernst effect of $\text{CsCa}_2\text{Fe}_4\text{As}_4\text{F}_2$, we separated the Nernst effect into two terms by using the following equation:

$$v = \left(\frac{\alpha_{xy}}{\sigma} - S \tan \theta \right) \frac{1}{B}. \quad (1)$$

The first term represents the off-diagonal Peltier coefficient divided by electrical conductance and magnetic field. In the second term, S and θ denote the thermopower and Hall angle, respectively, where $\tan \theta = \rho_{xy}/\rho_{xx}$. From the results shown in Fig. 4(b), the second term $-S \tan \theta/B$, represented by the hollow marks, is quite similar for the three systems in this

work. Meanwhile, it exhibits quite different features for the first term, indicated by the solid marks. For $\text{CsCa}_2\text{Fe}_4\text{As}_4\text{F}_2$, an obvious deviation emerges around 90 K in $\alpha_{xy}/\sigma B$, which is tagged by the red arrow. As the temperature decreases to 90 K, $\alpha_{xy}/\sigma B$ diverges from its initial moderate behavior and increases quickly. This phenomenon is absent in the other two systems, where $\alpha_{xy}/\sigma B$ of $\text{Ba}_{1-x}\text{K}_x\text{Fe}_2\text{As}_2$ and $\text{CaKFe}_4\text{As}_4$ are almost independent with temperature, exhibiting similar behaviors. Furthermore, comparing the terms $\alpha_{xy}/\sigma B$ and $-S \tan \theta/B$, they exhibit similar temperature dependence for $\text{Ba}_{1-x}\text{K}_x\text{Fe}_2\text{As}_2$ and $\text{CaKFe}_4\text{As}_4$, which implies the ‘‘Sondheimer cancellation’’ [34] is more complete in these two systems. In contrast, this cancellation is obviously violated for $\text{CsCa}_2\text{Fe}_4\text{As}_4\text{F}_2$ since a large disparity between $\alpha_{xy}/\sigma B$ and $-S \tan \theta/B$ is observed below 90 K. However, the off-diagonal Peltier coefficients α_{xy} of all three systems exhibit analogous behavior, as shown in the inset of Fig. 4(b). This may correspond to the aforementioned linear resistivity behavior, i.e., the resistivity becomes almost linearly temperature dependent as temperature decreases below 90 K for $\text{CsCa}_2\text{Fe}_4\text{As}_4\text{F}_2$. Therefore, the hump observed in the Nernst effect may correspond to the onset of linear resistivity, which may represent an incoherent-coherent crossover of charge dynamics. It is similar to the incoherent-coherent crossover observed in the resistivity of heavily doped AFe_2As_2 ($A = \text{K}, \text{Rb}, \text{Cs}$) [35,36].

Recently, the evidence of a pseudogap associated with preformed Cooper pairs was discovered for the two-dimensional superconductor $(\text{TBA})_x\text{FeSe}$ [16]. The large organic cluster TBA^+ inserts between the FeSe layer, which significantly increases its interlayer distance from $\sim 5.5 \text{ \AA}$, in pristine FeSe, to $\sim 15.5 \text{ \AA}$ [15,16]. Several experiments, including spin-lattice relaxation rate divided by temperature ($1/T_1T$) as well as the Knight shift (deviation from high temperature behavior around 60 K), magnetic susceptibility (deviation around 60 K), and Nernst effect (a broad hump below 65 K), all imply the existence of a pseudogap phenomenon and preformed Cooper pairs above its T_c ($\sim 43 \text{ K}$) in this unique two-dimensional superconductor [16]. By comparing these two-dimensional and quasi-two-dimensional superconductors of $(\text{TBA})_x\text{FeSe}$ and $\text{CsCa}_2\text{Fe}_4\text{As}_4\text{F}_2$, it is obvious that they share some similarities. $\text{CsCa}_2\text{Fe}_4\text{As}_4\text{F}_2$ also exhibits large resistivity anisotropy, reaching about 3150 around T_c [5], which is smaller than $(\text{TBA})_x\text{FeSe}$ ($\sim 10^5$ [16]) and significantly larger than BaFe_2As_2 (~ 150 [37] or ~ 6 [38]) and pristine FeSe (~ 4 [39]), suggesting $\text{CsCa}_2\text{Fe}_4\text{As}_4\text{F}_2$ is between three dimensional (3D) and 2D. Both of them exhibit an analogous broad peak of Nernst effect below T_c , because the vortex solid (Bragg lattice) is difficult to exist in a two-dimensional system. As for above T_c , they both reveal the unusual Nernst coefficients. However, unlike the pseudogap in $(\text{TBA})_x\text{FeSe}$ [16], the phenomenon is not obvious in $\text{CsCa}_2\text{Fe}_4\text{As}_4\text{F}_2$ and absent in $\text{Ba}_{1-x}\text{K}_x\text{Fe}_2\text{As}_2$ and $\text{CaKFe}_4\text{As}_4$. It may be a kind of Cooper pairing precursor for $\text{CsCa}_2\text{Fe}_4\text{As}_4\text{F}_2$ as the system evolves from 3D to quasi 2D. This is also consistent with the proposal that a two-dimensional nature helps to increase the temperature of the pairing gap based on the experiments of combined *in situ* electrical transport and ARPES of monolayer FeSe films grown on SrTiO_3 [40], which discovers that there exists a large pseudogap regime with

incoherent Cooper pairs above zero-resistance temperature. It explains the remarkable difference between the temperature of pairing gap detected by STS/ARPES experiments (higher than 60 K) [11–13] and the temperature of zero resistance obtained by transport measurements (below 40 K) [41–44].

Moreover, let us consider the possibility of Gaussian superconducting fluctuations [45] or electronic-nematic fluctuations [46] above T_c . However, there is a clear deviation, especially below ~ 80 K, when fitting the data to the Gaussian superconducting fluctuations (which is not shown here). As for the nematic fluctuations, the elastoresistance measurements show similar results for the three materials [30]. Meanwhile, our data of the Nernst effect and Hall effect exhibit a significant difference between the 12442-type material and the other two systems, against the elastoresistance experiments. Therefore, these two explanations may not be suitable for our results.

Then we compare the results of the NMR measurements for these three materials. In the NMR measurements, $1/T_1$ is related to the dynamic spin susceptibility with the following formula:

$$\frac{1}{T_1 T} \sim \sum_q \gamma_n^2 |A_\perp(q)|^2 \chi''(q, \omega) / \omega, \quad (2)$$

where χ'' is the q -dependent dynamic spin susceptibility, $A_\perp(q)$ is the transverse hyperfine form factor, γ_n is the nuclear gyromagnetic ratio, and ω is the Larmor frequency. Figures 5(a)–5(c) display the temperature dependence of $1/T_1 T$ of ^{75}As in $\text{CsCa}_2\text{Fe}_4\text{As}_4\text{F}_2$, $\text{CaKFe}_4\text{As}_4$ [47], and $\text{Ba}_{1-x}\text{K}_x\text{Fe}_2\text{As}_2$ [48]. The $1/T_1 T$ in $\text{CsCa}_2\text{Fe}_4\text{As}_4\text{F}_2$ has a clear enhancement with decreasing temperature, and displays a broad maximum around $T \sim 90$ K, suggesting the enhanced antiferromagnetic (AFM) fluctuation as similar to that in $\text{KCa}_2\text{Fe}_4\text{As}_4\text{F}_2$ [49]. Below 90 K, $1/T_1 T$ gradually decreases with further lowering of the temperature above the superconducting transition temperature $T_c \sim 28.5$ K. A similar behavior in $1/T_1 T$ is also observed in the ^{63}Cu NMR of underdoped cuprate superconductors (such as $\text{YBa}_2\text{Cu}_3\text{O}_{6.63}$ and $\text{Bi}_2\text{Sr}_2\text{CaCu}_2\text{O}_{8+\delta}$) which is ascribed to the pseudogap phenomenon in spin degree of freedom [50,51]. In contrast, the $1/T_1 T$ in $\text{CaKFe}_4\text{As}_4$ and $\text{Ba}_{1-x}\text{K}_x\text{Fe}_2\text{As}_2$ shows a monotonic increase with decreasing temperature and reaching the maximum around T_c , which indicates a persistent growth of AFM spin fluctuations [47,48]. Considering the similar differences in the Nernst and Hall effect, the reduction of the $1/T_1 T$ below about 90 K in $\text{CsCa}_2\text{Fe}_4\text{As}_4\text{F}_2$ is consistent with the proposed incoherent-coherent crossover picture or a kind of Cooper pairing precursor due to dimensional crossover in $\text{CsCa}_2\text{Fe}_4\text{As}_4\text{F}_2$.

IV. CONCLUSION

In conclusion, we have investigated transport, thermoelectric properties, and NMR of quasi-two-dimensional $\text{CsCa}_2\text{Fe}_4\text{As}_4\text{F}_2$, and also $\text{Ba}_{1-x}\text{K}_x\text{Fe}_2\text{As}_2$ and $\text{CaKFe}_4\text{As}_4$ for comparison, and discovered unusual features in the 12442-type system associated with its low-dimensional nature. In the superconducting state, the Nernst signals of both the 122- and 1144-type systems exhibit a sharp peak just below T_c which

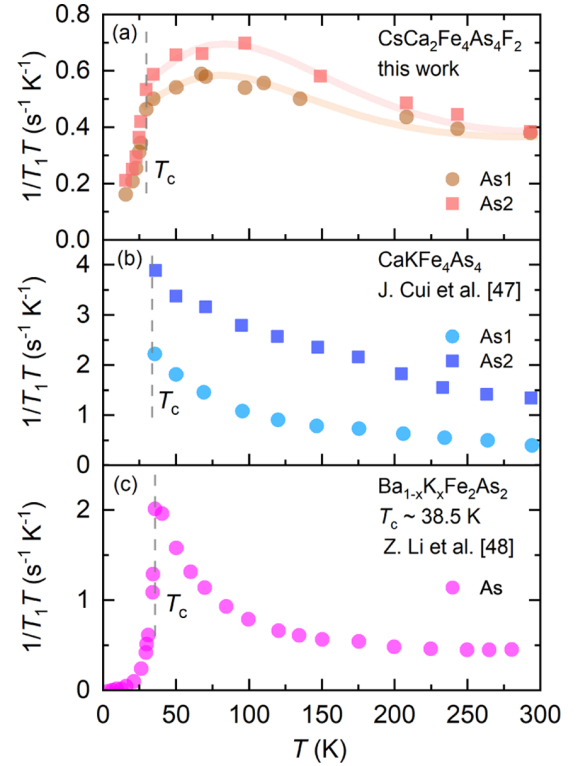


FIG. 5. (a)–(c) Temperature dependence of $1/T_1 T$ for $B \parallel c$ in $\text{CsCa}_2\text{Fe}_4\text{As}_4\text{F}_2$, $\text{CaKFe}_4\text{As}_4$, and $\text{Ba}_{1-x}\text{K}_x\text{Fe}_2\text{As}_2$ ($T_c \sim 38.5$ K). There are two types of As sites in $\text{CsCa}_2\text{Fe}_4\text{As}_4\text{F}_2$ ($\text{CaKFe}_4\text{As}_4$), namely, the As1 site which is close to the Cs (K) plane and the As2 site which is close to the Ca_2F_2 (Ca) block. Data for $\text{CaKFe}_4\text{As}_4$ and $\text{Ba}_{1-x}\text{K}_x\text{Fe}_2\text{As}_2$ from [47,48] are shown for comparison.

implies that there is only a narrow vortex-flowing regime in these two systems. Meanwhile, there may exist a large regime of the vortex liquid state for the 12442-type system, possibly connected to its quasi-two-dimensional nature. As for the temperatures above T_c , a hump in the Nernst coefficient is observed up to the temperature far above its T_c , around 90 K, in $\text{CsCa}_2\text{Fe}_4\text{As}_4\text{F}_2$, and correspondingly there is a clear suppression in the Hall coefficient in the same temperature range. Such abnormal features are absent in the other two systems which are more three dimensional. By further analyzing of the Nernst effect, the ‘‘Sondheimer cancellation’’ is not complete in the normal state of $\text{CsCa}_2\text{Fe}_4\text{As}_4\text{F}_2$. The unusual change in the Nernst and Hall effect, which coincides with the NMR measurement, may represent an incoherent-coherent crossover and/or a kind of Cooper pairing precursor for $\text{CsCa}_2\text{Fe}_4\text{As}_4\text{F}_2$ before it enters into the superconducting state. Apparently, such a phenomenon is not observed in the other two materials which are more three dimensional, thus we believe that these unusual precursor phenomena should result from the quasi-two-dimensional nature which is caused by the separated double FeAs layer. Combined with the observations of strong superconducting fluctuations in even more two-dimensional layered FeSe-based superconductors, this work demonstrates that the decreased dimensionality could have a significant impact on the superconductivity of iron-based superconductors.

ACKNOWLEDGMENTS

This work was supported by the National Key R&D Program of the China (Grant No. 2019YFA0308602), the National Science Foundation of China (Grant

No. 11774305), the Key R&D Program of Zhejiang Province in China (Grant No. 2021C01002), and the Fundamental Research Funds for the Central Universities of China.

- [1] Y. Kamihara, T. Watanabe, M. Hirano, and H. Hosono, Iron-based layered superconductor $\text{La}[\text{O}_{1-x}\text{F}_x]\text{FeAs}$ ($x = 0.05\text{-}0.12$) with $T_c = 26$ K, *J. Am. Chem. Soc.* **130**, 3296 (2008).
- [2] X.-H. Chen, T. Wu, G. Wu, R.-H. Liu, H. Chen, and D.-F. Fang, Superconductivity at 43 K in $\text{SmFeAsO}_{1-x}\text{F}_x$, *Nature (London)* **453**, 761 (2008).
- [3] M. Rotter, M. Tegel, and D. Johrendt, Superconductivity at 38 K in the Iron Arsenide $(\text{Ba}_{1-x}\text{K}_x)\text{Fe}_2\text{As}_2$, *Phys. Rev. Lett.* **101**, 107006 (2008).
- [4] Z.-C. Wang, C.-Y. He, S.-Q. Wu, Z.-T. Tang, Y. Liu, A. Ablimit, C.-M. Feng, and G.-H. Cao, Superconductivity in $\text{KCa}_2\text{Fe}_4\text{As}_4\text{F}_2$ with separate double Fe_2As_2 layers, *J. Am. Chem. Soc.* **138**, 7856 (2016).
- [5] Z.-C. Wang, Y. Liu, S.-Q. Wu, Y.-T. Shao, Z. Ren, and G.-H. Cao, Giant anisotropy in superconducting single crystals of $\text{CsCa}_2\text{Fe}_4\text{As}_4\text{F}_2$, *Phys. Rev. B* **99**, 144501 (2019).
- [6] S. Pyon, Y. Kobayashi, A. Takahashi, W. Li, T. Wang, G. Mu, A. Ichinose, T. Kambara, A. Yoshida, and T. Tamegai, Anisotropic physical properties and large critical current density in $\text{KCa}_2\text{Fe}_4\text{As}_4\text{F}_2$ single crystal, *Phys. Rev. Materials* **4**, 104801 (2020).
- [7] T. Wang, J. Chu, H. Jin, J. Feng, L. Wang, Y. Song, C. Zhang, W. Li, Z. Li, T. Hu, D. Jiang, W. Peng, X. Liu, and G. Mu, Single-crystal growth and extremely high H_{c2} of 12442-type Fe-based superconductor $\text{KCa}_2\text{Fe}_4\text{As}_4\text{F}_2$, *J. Phys. Chem. C* **123**, 13925 (2019).
- [8] D. Wu, W. Hong, C. Dong, X. Wu, Q. Sui, J. Huang, Q. Gao, C. Li, C. Song, H. Luo, C. Yin, Y. Xu, X. Luo, Y. Cai, J. Jia, Q. Wang, Y. Huang, G. Liu, S. Zhang, F. Zhang *et al.*, Spectroscopic evidence of bilayer splitting and strong interlayer pairing in the superconductor $\text{KCa}_2\text{Fe}_4\text{As}_4\text{F}_2$, *Phys. Rev. B* **101**, 224508 (2020).
- [9] D. L. Feng, N. P. Armitage, D. H. Lu, A. Damascelli, J. P. Hu, P. Bogdanov, A. Lanzara, F. Ronning, K. M. Shen, H. Eisaki, C. Kim, Z.-X. Shen, J.-i. Shimoyama, and K. Kishio, Bilayer Splitting in the Electronic Structure of Heavily Overdoped $\text{Bi}_2\text{Sr}_2\text{CaCu}_2\text{O}_{8+\delta}$, *Phys. Rev. Lett.* **86**, 5550 (2001).
- [10] W. Hong, L. Song, B. Liu, Z. Li, Z. Zeng, Y. Li, D. Wu, Q. Sui, T. Xie, S. Danilkin, H. Ghosh, A. Ghosh, J. Hu, L. Zhao, X. Zhou, X. Qiu, S. Li, and H. Luo, Neutron Spin Resonance in a Quasi-Two-Dimensional Iron-Based Superconductor, *Phys. Rev. Lett.* **125**, 117002 (2020).
- [11] Q.-Y. Wang, Z. Li, W.-H. Zhang, Z.-C. Zhang, J.-S. Zhang, W. Li, H. Ding, Y.-B. Ou, P. Deng, K. Chang, J. Wen, C.-L. Song, K. He, J.-F. Jia, S.-H. Ji, Y.-Y. Wang, L.-L. Wang, X. Chen, X.-C. Ma, and Q.-K. Xue, Interface-induced high-temperature superconductivity in single unit-cell FeSe films on SrTiO_3 , *Chin. Phys. Lett.* **29**, 037402 (2012).
- [12] S. He, J. He, W. Zhang, L. Zhao, D. Liu, X. Liu, D. Mou, Y.-B. Ou, Q.-Y. Wang, Z. Li, L. Wang, Y. Peng, Y. Liu, C. Chen, L. Yu, G. Liu, X. Dong, J. Zhang, C. Chen, Z. Xu *et al.*, Phase diagram and electronic indication of high-temperature superconductivity at 65 K in single-layer FeSe films, *Nat. Mater.* **12**, 605 (2013).
- [13] S. Tan, Y. Zhang, M. Xia, Z. Ye, F. Chen, X. Xie, R. Peng, D. Xu, Q. Fan, H. Xu, J. Jiang, T. Zhang, X. Lai, T. Xiang, J. Hu, B. Xie, and D. Feng, Interface-induced superconductivity and strain-dependent spin density waves in $\text{FeSe}/\text{SrTiO}_3$ thin films, *Nat. Mater.* **12**, 634 (2013).
- [14] M. Z. Shi, N. Z. Wang, B. Lei, C. Shang, F. B. Meng, L. K. Ma, F. X. Zhang, D. Z. Kuang, and X. H. Chen, Organic-ion-intercalated FeSe-based superconductors, *Phys. Rev. Materials* **2**, 074801 (2018).
- [15] M. Shi, N. Wang, B. Lei, J. Ying, C. Zhu, Z. Sun, J. Cui, F. Meng, C. Shang, L. Ma, and X. Chen, FeSe-based superconductors with a superconducting transition temperature of 50 K, *New J. Phys.* **20**, 123007 (2018).
- [16] B.-L. Kang, M.-Z. Shi, S.-J. Li, H.-H. Wang, Q. Zhang, D. Zhao, J. Li, D.-W. Song, L.-X. Zheng, L.-P. Nie, T. Wu, and X.-H. Chen, Preformed Cooper Pairs in Layered FeSe-Based Superconductors, *Phys. Rev. Lett.* **125**, 097003 (2020).
- [17] Z. A. Xu, N. P. Ong, Y. Wang, T. Kakeshita, and S.-i. Uchida, Vortex-like excitations and the onset of superconducting phase fluctuation in underdoped $\text{La}_{2-x}\text{Sr}_x\text{CuO}_4$, *Nature (London)* **406**, 486 (2000).
- [18] M. Matusiak, K. Rogacki, and T. Wolf, Thermoelectric anisotropy in the iron-based superconductor $\text{Ba}(\text{Fe}_{1-x}\text{Co}_x)_2\text{As}_2$, *Phys. Rev. B* **97**, 220501(R) (2018).
- [19] M. Matusiak and M. Babij, Thermoelectric signature of the nematic phase in hole-doped iron-based superconductors, *Phys. Rev. B* **99**, 174507 (2019).
- [20] M. Matusiak, M. Babij, and T. Wolf, Anisotropy of the Seebeck and Nernst coefficients in parent compounds of the iron-based superconductors, *Phys. Rev. B* **97**, 100506(R) (2018).
- [21] Y. Zheng, P. M. Tam, J. Hou, A. E. Böhmer, T. Wolf, C. Meingast, and R. Lortz, Absence of nematic order in the pressure-induced intermediate phase of the iron-based superconductor $\text{Ba}_{0.85}\text{K}_{0.15}\text{Fe}_2\text{As}_2$, *Phys. Rev. B* **93**, 104516 (2016).
- [22] L. Chen, Z. Xiang, C. Tinsman, B. Lei, X. Chen, G. D. Gu, and L. Li, Spontaneous Nernst effect in the iron-based superconductor $\text{Fe}_{1+y}\text{Te}_{1-x}\text{Se}_x$, *Phys. Rev. B* **102**, 054503 (2020).
- [23] K. Kihou, T. Saito, K. Fujita, S. Ishida, M. Nakajima, K. Horigane, H. Fukazawa, Y. Kohori, S.-i. Uchida, J. Akimitsu, A. Iyo, C.-H. Lee, and H. Eisaki, Single-crystal growth of $\text{Ba}_{1-x}\text{K}_x\text{Fe}_2\text{As}_2$ by KAs self-flux method, *J. Phys. Soc. Jpn.* **85**, 034718 (2016).
- [24] S. Ishida, A. Iyo, H. Ogino, H. Eisaki, N. Takeshita, K. Kawashima, K. Yanagisawa, Y. Kobayashi, K. Kimoto, H. Abe, M. Imai, J.-i. Shimoyama, and M. Eisterer, Unique defect structure and advantageous vortex pinning properties in superconducting $\text{CaKFe}_4\text{As}_4$, *npj Quantum Mater.* **4**, 27 (2019).
- [25] W. R. Meier, T. Kong, U. S. Kaluarachchi, V. Taufour, N. H. Jo, G. Drachuck, A. E. Böhmer, S. M. Saunders, A. Sapkota, A. Kreyssig, M. A. Tanatar, R. Prozorov, A. I. Goldman, F. F.

- Balakirev, A. Gurevich, S. L. Bud'ko, and P. C. Canfield, Anisotropic thermodynamic and transport properties of single-crystalline $\text{CaKFe}_4\text{As}_4$, *Phys. Rev. B* **94**, 064501 (2016).
- [26] K. Ohgushi and Y. Kiuchi, Doping dependence of Hall coefficient and evolution of coherent electronic state in the normal state of the Fe-based superconductor $\text{Ba}_{1-x}\text{K}_x\text{Fe}_2\text{As}_2$, *Phys. Rev. B* **85**, 064522 (2012).
- [27] Y. Liu and T. A. Lograsso, Crossover in the magnetic response of single-crystalline $\text{Ba}_{1-x}\text{K}_x\text{Fe}_2\text{As}_2$ and Lifshitz critical point evidenced by Hall effect measurements, *Phys. Rev. B* **90**, 224508 (2014).
- [28] B. Shen, H. Yang, Z.-S. Wang, F. Han, B. Zeng, L. Shan, C. Ren, and H.-H. Wen, Transport properties and asymmetric scattering in $\text{Ba}_{1-x}\text{K}_x\text{Fe}_2\text{As}_2$ single crystals, *Phys. Rev. B* **84**, 184512 (2011).
- [29] M. Gooch, B. Lv, B. Lorenz, A. M. Guloy, and C.-W. Chu, Evidence of quantum criticality in the phase diagram of $\text{K}_x\text{Sr}_{1-x}\text{Fe}_2\text{As}_2$ from measurements of transport and thermoelectricity, *Phys. Rev. B* **79**, 104504 (2009).
- [30] T. Terashima, Y. Matsushita, H. Yamase, N. Kikugawa, H. Abe, M. Imai, S. Uji, S. Ishida, H. Eisaki, A. Iyo, K. Kihou, C.-H. Lee, T. Wang, and G. Mu, Elastoresistance measurements on $\text{CaKFe}_4\text{As}_4$ and $\text{KCa}_2\text{Fe}_4\text{As}_4\text{F}_2$ with the Fe site of C_{2v} symmetry, *Phys. Rev. B* **102**, 054511 (2020).
- [31] M. Gooch, B. Lv, B. Lorenz, A. M. Guloy, and C. W. Chu, Critical scaling of transport properties in the phase diagram of iron pnictide superconductors $\text{K}_x\text{Sr}_{1-x}\text{Fe}_2\text{As}_2$ and $\text{K}_x\text{Ba}_{1-x}\text{Fe}_2\text{As}_2$, *J. Appl. Phys.* **107**, 09E145 (2010).
- [32] J. M. Harris, N. P. Ong, P. Matl, R. Gagnon, L. Taillefer, T. Kimura, and K. Kitazawa, Additive quasiparticle and vortex Hall conductivities in $\text{La}_{2-x}\text{Sr}_x\text{CuO}_4$ and untwinned $\text{YBa}_2\text{Cu}_3\text{O}_{6.93}$, *Phys. Rev. B* **51**, 12053(R) (1995).
- [33] Z.-W. Zhu, Z.-A. Xu, X. Lin, G.-H. Cao, C.-M. Feng, G.-F. Chen, Z. Li, J.-L. Luo, and N.-L. Wang, Nernst effect of a new iron-based superconductor $\text{LaO}_{1-x}\text{F}_x\text{FeAs}$, *New J. Phys.* **10**, 063021 (2008).
- [34] E. H. Sondheimer, The theory of the galvanomagnetic and thermomagnetic effects in metals, *Proc. R. Soc. London, Ser. A* **193**, 484 (1948).
- [35] Y. P. Wu, D. Zhao, A. F. Wang, N. Z. Wang, Z. J. Xiang, X. G. Luo, T. Wu, and X. H. Chen, Emergent Kondo Lattice Behavior in Iron-Based Superconductors AFe_2As_2 ($A = \text{K}, \text{Rb}, \text{Cs}$), *Phys. Rev. Lett.* **116**, 147001 (2016).
- [36] P. Wiecek, V. Taufour, D. Y. Chung, M. G. Kanatzidis, S. L. Bud'ko, P. C. Canfield, and Y. Furukawa, Pressure dependence of coherence-incoherence crossover behavior in KFe_2As_2 observed by resistivity and ^{75}As -NMR/NQR, *Phys. Rev. B* **97**, 064509 (2018).
- [37] X. F. Wang, T. Wu, G. Wu, H. Chen, Y. L. Xie, J. J. Ying, Y. J. Yan, R. H. Liu, and X. H. Chen, Anisotropy in the Electrical Resistivity and Susceptibility of Superconducting BaFe_2As_2 Single Crystals, *Phys. Rev. Lett.* **102**, 117005 (2009).
- [38] M. A. Tanatar, N. Ni, G. D. Samolyuk, S. L. Bud'ko, P. C. Canfield, and R. Prozorov, Resistivity anisotropy of AFe_2As_2 ($A = \text{Ca}, \text{Sr}, \text{Ba}$): Direct versus Montgomery technique measurements, *Phys. Rev. B* **79**, 134528 (2009).
- [39] S. I. Vedenev, B. A. Piot, D. K. Maude, and A. V. Sadakov, Temperature dependence of the upper critical field of FeSe single crystals, *Phys. Rev. B* **87**, 134512 (2013).
- [40] B. D. Faeth, S. L. Yang, J. K. Kawasaki, J. N. Nelson, P. Mishra, C. T. Parzyck, C. Li, D. G. Schlom, and K. M. Shen, Incoherent Cooper Pairing and Pseudogap Behavior in Single-Layer $\text{FeSe}/\text{SrTiO}_3$, *Phys. Rev. X* **11**, 021054 (2021).
- [41] W.-H. Zhang, Y. Sun, J.-S. Zhang, F.-S. Li, M.-H. Guo, Y.-F. Zhao, H.-M. Zhang, J.-P. Peng, Y. Xing, H.-C. Wang, T. Fujita, A. Hirata, Z. Li, H. Ding, C.-J. Tang, M. Wang, Q.-Y. Wang, K. He, S.-H. Ji, X. Chen, J.-F. Wang, Z.-C. Xia, L. Li, Y.-Y. Wang, J. Wang, L.-L. Wang, M.-W. Chen, Q.-K. Xue, and X.-C. Ma, Direct observation of high-temperature superconductivity in one-unit-cell FeSe films, *Chin. Phys. Lett.* **31**, 017401 (2014).
- [42] W. Zhang, Z. Li, F. Li, H. Zhang, J. Peng, C. Tang, Q. Wang, K. He, X. Chen, L. Wang, X. Ma, and Q.-K. Xue, Interface charge doping effects on superconductivity of single-unit-cell FeSe films on SrTiO_3 substrates, *Phys. Rev. B* **89**, 060506(R) (2014).
- [43] Y. Sun, W. Zhang, Y. Xing, F. Li, Y. Zhao, Z. Xia, L. Wang, X. Ma, Q.-K. Xue, and J. Wang, High temperature superconducting FeSe films on SrTiO_3 substrates, *Sci. Rep.* **4**, 6040 (2014).
- [44] Q. Wang, W. Zhang, Z. Zhang, Y. Sun, Y. Xing, Y. Wang, L. Wang, X. Ma, Q.-K. Xue, and J. Wang, Thickness dependence of superconductivity and superconductor-insulator transition in ultrathin FeSe films on $\text{SrTiO}_3(001)$ substrate, *2D Mater.* **2**, 044012 (2015).
- [45] I. Ussishkin, S. L. Sondhi, and D. A. Huse, Gaussian Superconducting Fluctuations, Thermal Transport, and the Nernst Effect, *Phys. Rev. Lett.* **89**, 287001 (2002).
- [46] R. Daou, J. Chang, D. LeBoeuf, O. Cyr-Choinière, F. Laliberté, N. Doiron-Leyraud, B. J. Ramshaw, R. Liang, D. A. Bonn, W. N. Hardy, and L. Taillefer, Broken rotational symmetry in the pseudogap phase of a high- T_c superconductor, *Nature (London)* **463**, 519 (2010).
- [47] J. Cui, Q. P. Ding, W. R. Meier, A. E. Böhmer, T. Kong, V. Borisov, Y. Lee, S. L. Bud'ko, R. Valentí, P. C. Canfield, and Y. Furukawa, Magnetic fluctuations and superconducting properties of $\text{CaKFe}_4\text{As}_4$ studied by ^{75}As NMR, *Phys. Rev. B* **96**, 104512 (2017).
- [48] Z. Li, D. L. Sun, C. T. Lin, Y. H. Su, J. P. Hu, and G.-Q. Zheng, Nodeless energy gaps of single-crystalline $\text{Ba}_{0.68}\text{K}_{0.32}\text{Fe}_2\text{As}_2$ as seen via ^{75}As NMR, *Phys. Rev. B* **83**, 140506(R) (2011).
- [49] J. Luo, C. Wang, Z. Wang, Q. Guo, J. Yang, R. Zhou, K. Matano, T. Oguchi, Z. Ren, G. Cao, and G.-Q. Zheng, NMR and NQR studies on transition-metal arsenide superconductors LaRu_2As_2 , $\text{KCa}_2\text{Fe}_4\text{As}_4\text{F}_2$, and $\text{A}_2\text{Cr}_3\text{As}_3$, *Chin. Phys. B* **29**, 067402 (2020).
- [50] M. Takigawa, A. P. Reyes, P. C. Hammel, J. D. Thompson, R. H. Heffner, Z. Fisk, and K. C. Ott, Cu and O NMR studies of the magnetic properties of $\text{YBa}_2\text{Cu}_3\text{O}_{6.63}$ ($T_c = 62$ K), *Phys. Rev. B* **43**, 247 (1991).
- [51] K. Ishida, K. Yoshida, T. Mito, Y. Tokunaga, Y. Kitaoka, K. Asayama, Y. Nakayama, J. Shimoyama, and K. Kishio, Pseudogap behavior in single-crystal $\text{Bi}_2\text{Sr}_2\text{CaCu}_2\text{O}_{8+\delta}$ probed by Cu NMR, *Phys. Rev. B* **58**, R5960(R) (1998).